This is a preprint, the final version is subject to change, of the American Mineralogist (MSA)
Cite as Authors (Year) Title. American Mineralogist, in press.
(DOI will not work until issue is live.) DOI: http://dx.doi.org/10.2138/am.2014.4441

REVISION 2

Oxy-dravite, $Na(Al_2Mg)(Al_5Mg)(Si_6O_{18})(BO_3)_3(OH)_3O$, a new mineral species of the tourmaline supergroup

FERDINANDO BOSI[1] AND HENRIK SKOGBY[2]

[1]Dipartimento di Scienze della Terra, Sapienza Università di Roma, P.le A. Moro, 5, I-00185 Rome, Italy

[2]Department of Mineralogy, Swedish Museum of Natural History, Box 50007, SE-10405 Stockholm, Sweden

ABSTRACT

Oxy-dravite, $Na(Al_2Mg)(Al_5Mg)(Si_6O_{18})(BO_3)_3(OH)_3O$, is a new mineral of the tourmaline supergroup. The holotype specimen originates from the locality of Osarara (Narok district, Kenya) and occurs in quartz-muscovite schist. Crystals of oxy-dravite are dark red, partially translucent with a vitreous luster, a pink streak and conchoidal fracture. It has a Mohs hardness of approximately 7, and a calculated density of 3.073 g/cm^3. In plane polarized light, oxy-dravite is pleochroic (O = orange and E = pink) and uniaxial negative: ω = 1.650(5), ε = 1.620(5). Oxy-dravite is rhombohedral, space group *R*3*m*, with the unit-cell parameters a = 15.9273(2) and c = 7.2001(1) Å, V = 1581.81(4) Å^3, Z = 3. Chemical characterization based on electron microprobe analysis, single-crystal structure refinement, Mössbauer and optical spectroscopy, resulted in the unit formula:

$^{X}(Na_{0.83}\square_{0.15}K_{0.02})_{\Sigma 1.00}\ ^{Y}(Al_{1.34}Fe^{3+}_{0.58}Mg_{1.03}Fe^{2+}_{0.03}Ti_{0.02})_{\Sigma 3.00}\ ^{Z}(Al_{4.95}Mg_{1.03}Fe^{3+}_{0.02})_{\Sigma 6.00}$ $^{T}(Si_{5.98}Al_{0.02}O_{18})_{\Sigma 6.00}\ ^{B}(BO_3)_3\ ^{V}(OH)_3\ ^{W}(O_{0.76}OH_{0.24})_{\Sigma 1.00}$.

While the end-member formula of oxy-dravite may be formalized as $Na^{Y}(Al_3)^{Z}(Al_4Mg_2)Si_6O_{18}(BO_3)_3(OH)_3O$, the most representative ideal structural formula is

$Na^{Y}(Al_2Mg)^{Z}(Al_5Mg)Si_6O_{18}(BO_3)_3(OH)_3O$. The difference between these two formulae is solely in Al-Mg order-disorder, i.e., there is no difference in chemical composition. Although the Mg-Al disorder over the *Y* and *Z* sites is controlled by the short-range bond-valence requirements of O^{2-} at the O1 (≡ W) site, the amount of Mg at the *Z* site is a function of the degree of cation size mismatch at Z.

The crystal structure of oxy-dravite was refined to statistical index *R*1 of 1.17% using 1586 equivalent reflections collected with Mo*K*α X-radiation. Oxy-dravite is chemically related to dravite (and fluor-dravite), $NaMg_3Al_6Si_6O_{18}(BO_3)_3(OH)_3(OH,F)$, by the heterovalent substitution $Al^{3+} + O^{2-} \rightarrow Mg^{2+} + (OH,F)^{1-}$.

INTRODUCTION

The tourmaline supergroup minerals are widespread, occurring in a wide variety of sedimentary, igneous and metamorphic rocks. They are known as valuable indicator minerals that can provide information on the compositional evolution of their host rocks, chiefly due to their ability to incorporate a large number of elements (e.g., Novák et al. 2004; Agrosì et al. 2006; Lussier et al. 2011a; Novák et al. 2011; van Hinsberg et al. 2011). However, the chemical composition of tourmalines is also strongly controlled by various crystal-structural constraints (e.g., Hawthorne 1996, 2002a; Bosi 2010, 2011; Henry and Dutrow 2011; Skogby et al. 2012) as well as by temperature (e.g., van Hinsberg and Schumacher 2011). Tourmaline supergroup minerals are complex borosilicates and their crystal structure and crystal chemistry have been widely studied (e.g., Foit 1989; Hawthorne and Henry 1999; Bosi and Lucchesi 2007; Lussier et al. 2008; Bosi et al. 2010; Lussier et al. 2011b). In accordance with Henry et al. (2011), the general formula of tourmaline may be written as: $XY_3Z_6T_6O_{18}(BO_3)_3V_3W$, where X (≡ $^{[9]}X$) = Na^{+}, K^{+}, Ca^{2+}, □ (= vacancy); Y (≡ $^{[6]}Y$) = Al^{3+}, Fe^{3+}, Cr^{3+}, V^{3+}, Mg^{2+}, Fe^{2+}, Mn^{2+}, Li^{+}; Z (≡ $^{[6]}Z$) = Al^{3+}, Fe^{3+}, Cr^{3+}, V^{3+}, Mg^{2+}, Fe^{2+}; T (≡ $^{[4]}T$) = Si^{4+}, Al^{3+}, B^{3+}; B (≡ $^{[3]}B$) = B^{3+}; W (≡ $^{[3]}$O1) = OH^{1-}, F^{1-}, O^{2-}; V (≡ $^{[3]}$O3) = OH^{1-}, O^{2-} and where, for example, T represents a group of cations (Si^{4+}, Al^{3+}, B^{3+}) accommodated at the [4]-coordinated *T* sites. The dominance of these ions at one or more sites of the structure gives rise to a range of distinct mineral species (Henry et al. 2011).

The name oxy-dravite was first proposed by Hawthorne and Henry (1999) for the hypothetical formula:

$$Na^{Y}(Al_2Mg)^{Z}(Al_5Mg)Si_6O_{18}(BO_3)_3(OH)_3O \quad (1)$$

Successively the name was confirmed in the approved classification scheme of Henry et al. (2011), but with a new ideal formula:

$$Na^{Y}(Al_3)^{Z}(Al_4Mg_2)Si_6O_{18}(BO_3)_3(OH)_3O \quad (2)$$

Although these two structural formulas are chemically equivalent, formula (1) shows a disordering of Mg over the *Y* and *Z* sites, whereas formula (2) shows an ordering of Mg at the *Z* site. As these two structural formulae show long-range disordered (1) and long-range ordered site populations (2) for the bulk composition $NaMg_2Al_7Si_6O_{18}(BO_3)_3(OH)_3O$, we define (1) as the disordered formula and (2) as the ordered formula. The name oxy-dravite has been previously used for some time in the literature despite the lack of a formal definition of the mineral (e.g., Žáček et al. 2000; Novák et al. 2004; Bosi et al. 2010).

The new species as well as the name have been approved by the Commission on New Minerals, Nomenclature and Classification of the International Mineralogical Association (IMA 2012-004a). The holotype specimen of oxy-dravite is deposited in the collections of the Museum of Mineralogy, Earth Sciences Department, Sapienza University of Rome, Italy, catalogue number 33066. A formal description of the new species oxy-dravite is presented here, including a full characterization of its physical, chemical and structural attributes.

OCCURRENCE, APPEARANCE AND PHYSICAL AND OPTICAL PROPERTIES

The holotype specimen originates from the locality of Osarara (Narok district, Kenya), and occurs in quartz-muscovite schist (Dunn et al. 1975). The crystal is inclusion-free and occurs as an euhedral crystal approximately $7 \times 7 \times 15$ mm in size. It is dark red in color, with pink streak, partially translucent and has a vitreous luster (Fig. 1). It is brittle and shows conchoidal fracture. The Mohs hardness is approximately 7 and the calculated density is 3.073 g/cm^3. In transmitted light, oxy-dravite is pleochroic with O = orange and E = pink. Oxy-dravite is uniaxial negative with refractive indices, measured by the immersion method using white light from a tungsten source, of ω = 1.650(5), ε = 1.620(5). The mean index of refraction, density and chemical composition lead to a compatibility index of 0.020, classed as excellent (Mandarino 1976, 1981).

It is worth pointing out that the dark red bulk color as well as the pleochroism observed is most likely caused by relatively minor concentrations of Fe^{3+} present in the mineral (Taran and Rossman 2002).

EXPERIMENTAL METHODS

Single-crystal structural refinement (SREF)

A representative fragment of the type specimen was selected for X-ray diffraction measurements on a Bruker KAPPA APEX-II single-crystal diffractometer, at Sapienza University of Rome (Earth Sciences Department), equipped with a CCD area detector (6.2 × 6.2 cm^2 active detection area, 512 × 512 pixels) and a graphite crystal monochromator, using Mo*K*α radiation from a fine-focus sealed X-ray tube. The sample-to-detector distance was 4 cm. A total of 3265 exposures (step = 0.2°, time/step = 20 s) covering the full reciprocal sphere with a high redundancy of about 8 was used. Final unit-cell parameters were refined by means of the Bruker AXS SAINT program using reflections with $I > 10\ \sigma(I)$ in the range $8° < 2\theta < 69°$. The intensity data were processed and corrected for Lorentz, polarization, and background effects with the APEX2 software program of Bruker AXS. The data were corrected for absorption using the multi-scan method (SADABS). The absorption correction led to a significant improvement in R_{int} (from 0.0363 to 00266). No violations of *R*3*m* symmetry were noted.

Structural refinement was carried out with the SHELXL-97 program (Sheldrick 2008). Starting coordinates were taken from Bosi and Lucchesi (2004). Variable parameters that were refined include: scale factor, extinction coefficient, atomic coordinates, site scattering values and atomic displacement factors. To obtain the best values of statistical indexes (*R*1, *wR*2), a fully ionized O scattering curve was used, whereas neutral scattering curves were used for the other atoms. In detail, the *X* site was modeled using Na scattering factors. The occupancy of the *Y* site was obtained considering the presence of Al vs. Fe. The *Z*, *T* and *B* sites were modeled, respectively, with Al, Si and B scattering factors and with a fixed occupancy of 1, because refinement with unconstrained occupancies showed no significant deviations from this value. Three full-matrix refinement cycles with isotropic displacement parameters for all atoms were followed by anisotropic cycles until convergence was attained. No significant correlations over a value of 0.7 between the parameters were observed at the end of

refinement. Table 1 lists crystal data, data collection information and refinement details; Table 2 gives the fractional atomic coordinates and site occupancies; Table 3 gives the displacement parameters; Table 4 gives selected bond distances.

X-ray powder diffraction

The X-ray powder-diffraction pattern for the oxy-dravite sample was collected using a Panalytical X'pert powder diffractometer equipped with an X'celerator silicon-strip detector. The range 5-80º (2θ) was scanned with a step-size of 0.017º during 30 minutes using a sample spinner with the sample mounted on a background-free holder. The diffraction data (in Å for CuK, λ_1 = 1.54060 Å), corrected using Si as an internal standard, are listed in Table 5. Unit-cell parameters from the powder data were refined using the program UnitCell (Holland and Redfern 1997): a = 15.919(1) Å, c = 7.200(1) Å, V = 1580.3(1) Å^3.

Electron Microprobe analysis (EMPA)

Electron microprobe analyses of the crystal used for X-ray diffraction refinements were obtained by using wavelength-dispersive spectrometry with a Cameca SX50 instrument at the "Istituto di Geologia Ambientale e Geoingegneria (Rome, Italy), CNR", operating at an accelerating potential of 15 kV and a sample current of 15 nA (5 μm beam diameter). Minerals and synthetic compounds were used as standards: wollastonite (Si*K*α, Ca*K*α), magnetite (Fe*K*α), rutile (Ti*K*α), corundum (Al*K*α), fluorphlogopite (F*K*α), periclase (Mg*K*α), jadeite (Na*K*α), K-feldspar (K*K*α), sphalerite (Zn*K*α), along with metallic Cr, V, Mn and Cu. The PAP matrix correction procedure (Pouchou and Pichoir 1991) was applied to reduce the raw data. The results, which are summarized in Table 5, represent mean values of 10 spot analyses. In accordance with the documented very low concentration of Li in dravitic samples (e.g., Henry et al. 2011), the Li_2O content was assumed to be insignificant. Manganese, Cr, V, Zn, Cu, Ca and F were found to be below their respective detection limits varying between 0.03 wt. % and 0.05 wt. %.

Mössbauer spectroscopy (MS)

The oxidation state of Fe was determined by Mössbauer spectroscopy at room temperature using a conventional spectrometer system operating in constant-acceleration mode. In order to spare the holotype material, the absorber was prepared by filling a small

quantity of ground material in a 1-mm hole in a lead plate, and the spectrum then acquired using a closely positioned ^{57}Co point-source in rhodium matrix with a nominal activity of 10 mCi. The spectrum was calibrated against α-Fe foil and folded before fitting using the MDA software by Jernberg and Sundqvist (1983). The resultant spectrum (Fig. 2) shows a relatively broad central absorption doublet with weak shoulder features. On a sample of similar composition from Osarara, Narok district, Kenya (NMNH#126030), Mattson and Rossman (1984) obtained a comparable spectrum and interpreted the broad bands as being caused by relaxation effects. The spectrum of the holotype specimen was fitted with two bands assigned to Fe^{3+} and one band assigned to Fe^{2+}, resulting in an $Fe^{3+}/\Sigma Fe$ ratio of approximately 0.96.

Optical spectroscopy (OAS)

Polarized room temperature optical absorption spectra in the ε and ω directions were recorded on a 31 μm thick crystal section in the UV/VIS to NIR spectral range (330-1500 nm) with a Zeiss MPM800 microscope spectrometer (cf. Halenius et al. 2011). The obtained spectra (not shown here) are very similar to those reported by Mattson and Rossman (1984) and Taran and Rossman (2002) for the NMNH#126030 sample, showing three absorption bands at 486, 540 and 545 nm related to Fe^{3+}-Fe^{3+} pair transitions and two Fe^{2+} bands around 700 and 1100 nm (Taran and Rossman 2002).

RESULTS

Determination of atomic proportions

In agreement with the structural refinement results, the boron content was assumed to be stoichiometric in the sample of oxy-dravite (B = 3.00 atoms per formula unit, apfu). In fact, both the site-scattering results and the bond lengths of *B* and *T* are consistent with the *B* site fully occupied by boron, but along with it being absent at the *T* site. The OH content can then be calculated by charge balance with the assumption ($T + Y + Z$) = 15.00. The atomic proportions were calculated on this assumption (Table 5). The excellent match between the number of electrons per formula unit (epfu) derived from chemical and structural analysis supports this procedure: 231.8 epfu vs. 232.8 epfu, respectively.

Site populations

Anion site populations were apportioned following the protocols of Grice and Ercit (1993) and Henry et al. (2011): the O3 site (V position in the general formula) is occupied by OH and O^{2-}, while the O1 site (W position in the general formula) is occupied by O^{2-} and OH. The cation distribution at the *T*, *Y* and *Z* sites was optimized by using a quadratic program (for details, see Bosi and Lucchesi 2004) to minimize the residuals between calculated and observed data (based on the chemical and structural analysis). Site scattering values, octahedral and tetrahedral mean bond distances (i.e., <*Y*-O>, <*Z*-O> and <*T*-O>) were calculated as the linear contribution of each cation multiplied by its specific bond distance (Table 6). More details about the specific distances derived from the ionic radii are found in Bosi and Lucchesi (2007). The robustness of this approach was confirmed by another optimization procedure (Wright et al. 2000) which led to very similar cation distributions in the present sample (Table 6). This result represents another example of convergence of these two procedures to similar solutions for tourmaline (i.e., Bosi and Lucchesi 2007; Filip et al. 2012; Bosi et al. 2012; Bosi et al. 2013).

The empirical structural formula of oxy-dravite is:

$^{X}(Na_{0.83}\square_{0.15}K_{0.02})_{\Sigma 1.00}\,^{Y}(Al_{1.34}Fe^{3+}_{0.58}Mg_{1.03}Fe^{2+}_{0.03}Ti_{0.02})_{\Sigma 3.00}\,^{Z}(Al_{4.95}Mg_{1.03}Fe^{3+}_{0.02})_{\Sigma 6.00}$
$^{T}(Si_{5.98}Al_{0.02}O_{18})_{\Sigma 6.00}\,^{B}(BO_3)_3\,^{V}(OH)_3\,^{W}(O_{0.76}OH_{0.24})_{\Sigma 1.00}$.

The results from bond-valence analysis are also consistent with the proposed structural formula. Bond valence calculations, using the formula and bond-valence parameters from Brown and Altermatt (1985), are reported in Table 7. In particular, note that the value of bond valence sum incident at the O1 site (1.53 valence units) implies that O1 (≡ W) is only partially occupied by an OH group (expected value close to 1). This is consistent with O^{2-} being dominant at the O1 site (expected value close to 2). This finding can be verified by means of the empirical relation reported in the CNMNC-approved proposal IMA 2012-004a by Bosi and Skogby, in which the OH content at O1 in tourmaline can be estimated by considering the bond valence sum at O1 and the F content according to: $^{W}OH = [2 - BVS(O1) - 0.20 - F]$. The resulting value (0.27 apfu) is very close to the OH value obtained by stoichiometry (0.24 apfu). It is noteworthy that the very small amounts of Fe^{3+} at the *Z* site (0.02 apfu) optimized in the structural formula are in good agreement with the presence of Fe^{3+} at *Z* observed in the polarized optical absorption spectrum of oxy-dravite samples from Osarara, with a band at 540

225 nm (**E** parallel to the **c** axis) assigned to electronic $^{Z}Fe^{3+}$-$^{Z}Fe^{3+}$ pair transitions (Mattson and
226 Rossman 1984; Taran and Rossman 2002).
227
228
229 ## DISCUSSION
230
231 ### Red tourmalines
232 Although not previously classified as oxy-dravite, unusual red Fe^{3+}-rich tourmalines
233 from Osarara (Narok district, Kenya) have been previously studied by different techniques, in
234 order to define the chemistry, the structure and the interactions between and among ions in the
235 atomic sites (Dunn et al. 1975, EMPA; Mattson and Rossman 1984, EMPA, MS and OAS;
236 Hawthorne et al. 1993, EMPA and SREF; Taran and Rossmann 2002, OAS). However, some
237 differences occur with respect to the data obtained for the holotype specimen: for example, the
238 unit-cell parameters are a =15.9273(2) and c = 7.2001(1) Å in our sample, and a =15.947(2)
239 and c = 7.214(1) Å in Hawthorne et al. (1993). Moreover, although the structural formula
240 reported by Hawthorne et al. (1993) shows a cation site populations quite similar to that of our
241 sample, the anion site populations at O3 and O1 were not specified, since the atomic
242 proportions were calculated by the assumption $^{V+W}(OH+F) = 4.00$ apfu, instead of the more
243 appropriate assumption ($T + Y + Z$) = 15.00 apfu. The latter assumption implies: 1) no
244 vacancies at the octahedrally-coordinated sites in line with the crystal structure information
245 and 2) a site population at O1 in line with the bond-valence sum value incident at the O1 site
246 (~1.5 valence units). As a result, the anion population is $^{W}(O_{0.69}OH_{0.31})$. It is noteworthy that
247 the anion population is consistent with the short-range bond-valence constrains around O1,
248 thus implying that the Mg-Al disorder over the Y and Z sites should be coupled to the
249 incorporation of O^{2-} at the O1 site (e.g., Taylor et al. 1995; Hawthorne 1996).
250
251 ### Nomenclature
252 The empirical structural formula of the sample examined in this study indicates this
253 tourmaline-supergroup mineral is best classed in the alkali group, oxy-subgroup 3 (Henry et al.
254 2011) with Na dominant at the X position of the general formula, oxygen dominant at the W
255 position with O^{2-} > OH, and Al as the dominant cation at the Y and Z positions. Disregarding
256 the minor constituents (K, Fe^{2+} and Ti and ^{T}Al) and replacing (+ OH^{-}) by (Na^{+} + O^{2-}) and

Fe^{3+} by Al, the empirical structural formula of the studied tourmaline can be approximated as $Na^{Y}(Al_2Mg)^{Z}(Al_5Mg)Si_6O_{18}(BO_3)_3(OH)_3O$, that is, one having a disordered formula (1). As this composition has multiple cations at more than one site (i.e., Al and Mg), it is not in accordance with the characteristics of an ordered end-member formula as defined by Hawthorne (2002b).

End-member formula

The empirical formula presented above can be rearranged to the two possible end-members: $Na^{Y}(AlMg_2)^{Z}(Al_6)Si_6O_{18}(BO_3)_3(OH)_3O$ and $Na^{Y}(Al_3)^{Z}(Al_4Mg_2)Si_6O_{18}(BO_3)_3(OH)_3O$.

In accordance with the short-range bond-valence requirements at O1 (e.g., Hawthorne 1996), however, the end-member with Mg ordered at Y would suggest the existence of an unstable short-range arrangement $^{Y}(Al + 2Mg)\text{-}^{W}(O^{2-})$ in oxy-dravite, whereas the end-member with Mg ordered at Z is both consistent with the occurrence of the stable short-range arrangement $^{Y}(3Al)\text{-}^{W}(O^{2-})$ and with the characteristics of an end-member composition (Hawthorne 2002b). Consequently, the $Na^{Y}(Al_3)^{Z}(Al_4Mg_2)Si_6O_{18}(BO_3)_3(OH)_3O$ formula is preferred as the end-member oxy-dravite composition. Finally, note that both the disordered formula (1) and the empirical formula are consistent with the stable short-range arrangement $^{Y}(2Al + Mg)\text{-}^{W}(O^{2-})$ (Hawthorne 1996).

Name and relation to other species

By analogy to the relationship between oxy-schorl and schorl (Bačík et al. 2013), oxy-chromium-dravite and chromium-dravite (Bosi et al. 2012), oxy-vanadium-dravite and "vanadium-dravite" (Bosi et al. 2013), the name oxy-dravite is given in relation to dravite. The prefix *oxy* represents the heterovalent substitution $Al^{3+} + O^{2-} \rightarrow Mg^{2+} + (OH)^{1-}$ relative to the root composition of dravite. Replacing (OH) by F in the above heterovalent substitution, also suggests a relationship between oxy-dravite and fluor-dravite, the latter being the fluor-equivalent of dravite (Clark et al. 2011). Comparative data for oxy-dravite, fluor-dravite and dravite are given in Table 8. Ideally, oxy-dravite is related to oxy-schorl, oxy-chromium-dravite, oxy-vanadium-dravite and povondraite through the homovalent substitution of Mg^{2+} for Fe^{2+}, Al^{3+} for Cr^{3+}, Al^{3+} for V^{3+} and Al^{3+} for Fe^{3+}, respectively (Table 9).

Mg-Al disorder

It must be stressed that the difference between the ordered and disordered formula being considered for oxy-dravite wholly relates Mg-Al order-disorder and does not impact on the resulting chemical composition. The two atoms of Mg can be disordered over the *Y* and *Z* sites, or fully ordered at *Z* as occurs in the other oxy(O1)-tourmalines such as oxy-chromium-dravite and oxy-vanadium-dravite (Table 9). In this regard, several empirical structural formulae of oxy-dravite reported in the literature approach $Na^{Y}(Al_2Mg)^{Z}(Al_5Mg)Si_6O_{18}(BO_3)_3(OH)_3O$ (e.g., Bloodaxe et al. 1999; Bosi and Lucchesi, 2004, 2007; Bosi et al. 2010) rather than the end-member proposed herein. The occurrence of Mg at the *Z* site and Al at the *Y* site is commonly coupled to the occurrence of O^{2-} at the O1 site, controlled by the relationship $2^{Y}Mg^{2+} + {}^{Z}Al^{3+} + {}^{W}(OH)^{1-} \leftrightarrow 2^{Y}Al^{3+} + {}^{Z}Mg^{2+} + {}^{W}O^{2-}$ (Hawthorne 1996). This relationship has been generalized as $3^{Y}Mg^{2+} + 2^{Z}Al^{3+} + {}^{W}(OH)^{1-} \leftrightarrow 3^{Y}Al^{3+} + 2^{Z}Mg^{2+} + {}^{W}O^{2-}$ by Henry *et al*. (2011) on the basis of findings of Bosi and Lucchesi (2007), namely that a maximum of 2 divalent cations (i.e., $Mg^{2+} + Fe^{2+}$) per formula unit can occur at the *Z* site. The latter authors, however, based their findings on Al-poor tourmalines, in which the Al is substituted by ions with larger ionic radius (e.g., Fe^{3+} and Cr). Actually, the amounts of Mg at *Z* are a product of the mismatch in size of cations occupying the Z-site; in fact, this mismatch is larger when involving Mg-Al rather than Mg-Cr^{3+} or Mg-V^{3+} as the ionic radii of ${}^{Z}Cr^{3+}$ (0.613 Å) or ${}^{Z}V^{3+}$ (0.653 Å) are much larger than that of ${}^{Z}Al$ (0.543 Å) (Bosi and Lucchesi 2007). Figure 3 displays the increase of ΣR^{2+} at *Z* (such as Mg and Fe^{2+}) as a function of replacement of ΣAl at *Y* and *Z* by larger cations like V^{3+}, Cr^{3+} and Fe^{3+} in tourmalines, showing that the amounts of Mg at the *Z* site is dependent on the R^{3+}-cation size. These observations strongly support the concept that Mg is distributed over the *Y* and *Z* sites in Al-rich oxy(O1)-tourmalines. Note that although the occurrence of Fe^{2+} at *Z* seems to be limited to Fe^{3+}-bearing Al-rich tourmalines (e.g., Filip et al 2012), Mg is observed as to be the only divalent cation occurring at the *Z* site in Al-poor tourmalines (e.g., Bosi et al 2004, 2012, 2013).

CONCLUDING REMARKS

Some important characteristics of oxy-dravite are:

1) the end-member formula is: $Na^{Y}(Al_3)^{Z}(Al_4Mg_2)Si_6O_{18}(BO_3)_3(OH)_3O$;

2) the most representative ideal formula is: $Na^{Y}(Al_2Mg)^{Z}(Al_5Mg)Si_6O_{18}(BO_3)_3(OH)_3O$;
3) the Mg-Al disorder over the *Y* and *Z* sites is controlled by the short-range bond-valence requirements of O^{2-} at O1;
4) the amount of Mg at the *Z* site is a function of the degree of cation size mismatch at Z.

ACKNOWLEDGMENTS

We thank Ulf Hålenius for his kind assistance in the collection and interpretation of optical absorption spectra. Chemical analyses were carried out with the kind assistance of M. Serracino to whom the authors express their gratitude. We also thank the AE A. McDonald for his useful suggestions that improved the quality of the manuscript.

REFERENCES CITED

Agrosì, G., Bosi, F., Lucchesi, S., Melchiorre, G., and Scandale, E. (2006) Mn-tourmaline crystals from island of Elba (Italy): Growth history and growth marks. American Mineralogist, 91, 944-952.

Bačík, P., Cempírek, J., Uher, P., Novák, M., Ozdín, D., Filip, J., Škoda, R., Breiter, K., Klementová, M., and Ďuďa R. (2013) Oxy-schorl, $Na(Fe^{2+}_2Al)Al_6Si_6O_{18}(BO_3)_3(OH)_3O$, a new mineral from Zlatá Idka, Slovak Republic and Přibyslavice, Czech Republic. American Mineralogist. Doi.org/10.2138/am.2013.4293.

Bloodaxe, E.S., Hughes, J.M., Dyar, M.D., Grew, E.S., and Guidotti, C.V. (1999) Linking structure and chemistry in the schorl-dravite series. American Mineralogist, 84, 922.928.

Bosi, F. (2008) Disordering of Fe^{2+} over octahedrally coordinated sites of tourmaline. American Mineralogist, 93, 1647-1653.

Bosi, F. (2010) Octahedrally coordinated vacancies in tourmaline: a theoretical approach. Mineralogical Magazine, 74, 1037-1044.

Bosi, F. (2011) Stereochemical constraints in tourmaline: from a short-range to a long-range structure. Canadian Mineralogist, 49, 17-27.

Bosi, F. and Lucchesi, S. (2004) Crystal chemistry of the schorl-dravite series. European Journal of Mineralogy, 16, 335-344.

Bosi, F. and Lucchesi, S. (2007) Crystal chemical relationships in the tourmaline group: structural constraints on chemical variability. American Mineralogist, 92, 1054-1063.

Bosi F., Lucchesi, S., and Reznitskii, L. (2004) Crystal chemistry of the dravite-chromdravite series. European Journal of Mineralogy, 16, 345-352.

Bosi, F., Balić-Žunić, T., and Surour, A.A. (2010) Crystal structure analysis of four tourmalines from the Cleopatra's Mines (Egypt) and Jabal Zalm (Saudi Arabia), and the role of Al in the tourmaline group. American Mineralogist, 95, 510-518.

Bosi, F., Reznitskii, L., and Skogby, H. (2012) Oxy-chromium-dravite, $NaCr_3(Cr_4Mg_2)(Si_6O_{18})(BO_3)_3(OH)_3O$, a new mineral species of the tourmaline supergroup. *American Mineralogist*, 97, 2024-2030.

Bosi, F., Reznitskii, L., and Sklyarov, E.V. (2013) Oxy-vanadium-dravite, $NaV_3(V_4Mg_2)(Si_6O_{18})(BO_3)_3(OH)_3O$: crystal structure and redefinition of the "vanadium-dravite" tourmaline. American Mineralogist, 98, 501-505.

Brown, I.D. and Altermatt, D. (1985) Bond-valence parameters obtained from a systematic analysis of the Inorganic Crystal Structure Database. Acta Crystallographica, B41, 244-247.

Clark, C.M., Hawthorne, F.C., and Ottolini, L. (2011) Fluor-dravite, $NaMg_3Al_6Si_6O_{18}(BO_3)_3(OH)_3F$, a new mineral species of the tourmaline group from the Crabtree emerald mine, Mitchell County, North Carolina: description and crystal structure.

Dunn, P.J., Arem, J.E. and Saul, J. (1975) Red dravite from Kenya. Journal of Gemmology, 14, 386-387.

Filip, J., Bosi, F., Novák, M., Skogby, H., Tuček, J., Čuda, J., and Wildner, M. (2012) Redox processes of iron in the tourmaline structure: example of the high-temperature treatment of Fe^{3+}-rich schorl. Geochimica et Cosmochimica Acta, 86, 239-256.

Foit, F.F. Jr. (1989) Crystal chemistry of alkali-deficient schorl and tourmaline structural relationships. American Mineralogist, 74, 422-431.

Grice, J.D. and Ercit, T.S. (1993) Ordering of Fe and Mg in the tourmaline crystal structure: the correct formula. Neues Jahrbuch für Mineralogie, Abhandlungen, 165, 245-266.

Jernberg, P. and Sundqvist, T. (1983) A versatile Mössbauer analysis program. Uppsala University, Institute of Physics (UUIP-1090).

Hålenius, U., Bosi, F. and Skogby, H. (2011) Structural relaxation of MnO_4 polyhedra in the spinel-galaxite solid solution. American Mineralogist, 96, 617-622.

Hawthorne, F.C. (1996) Structural mechanisms for light-element variations in tourmaline. Canadian Mineralogist, 34, 123-132.

Hawthorne, F.C. (2002a) Bond-valence constraints on the chemical composition of tourmaline. Canadian Mineralogist, 40, 789-797.

Hawthorne, F.C. (2002b) The use of end-member charge-arrangements in defining new mineral species and heterovalent substitutions in complex minerals. Canadian Mineralogist, 40, 699-710.

Hawthorne, F.C. and Henry, D. (1999) Classification of the minerals of the tourmaline group. European Journal of Mineralogy, 11, 201-215.

Hawthorne, F.C., MacDonald, D.J., and Burns, P.C. (1993) Reassignment of cation occupancies in tourmaline: Al-Mg disorder in the crystal structure of dravite. American Mineralogist, 78, 265.270.

Henry, D.J. and Dutrow, B.L. (2011) The incorporation of fluorine in tourmaline: Internal crystallographic controls or external environmental influences? Canadian Mineralogist, 49, 41–56.

Henry, D.J., Novák, M., Hawthorne, F.C., Ertl, A., Dutrow, B., Uher, P., and Pezzotta, F. (2011) Nomenclature of the tourmaline supergroup minerals. American Mineralogist, 96, 895-913.

Holland, T.J.B. and Redfern, S.A.T. (1997) Unit cell refinement from powder diffraction data: the use of regression diagnostics. Mineralogical Magazine, 61, 65-77.

Lussier, A.J., Aguiar, P.M., Michaelis, V.K., Kroeker, S., Herwig, S., Abdu, Y., and Hawthorne, F.C. (2008) Mushroom elbaite from the Kat Chay mine, Momeik, near Mogok, Myanmar: I. Crystal chemistry by SREF, EMPA, MAS NMR and Mössbauer spectroscopy. Mineralogical Magazine, 72, 747-761.

Lussier, A.J., Hawthorne, F.C., Aguiar, P.M., Michaelis, V.K., and Kroeker, S. (2011a) Elbaite-liddicoatite from Black Rapids glacier, Alaska. Periodico di Mineralogia, 80, 57-73.

Lussier, A.J., Abdu, Y. Hawthorne, F.C., Michaelis, V.K., Aguiar, P.M., and Kroeker, S. (2011b) Oscillatory zoned liddicoatite from Anjanabonoina, central Madagascar. I. Crystal chemistry and structure by SREF and ^{11}B and ^{27}Al MAS NMR spectroscopy. Canadian Mineralogist, 49, 63-88.

Mandarino, J.A. (1976) The Gladstone-Dale relationship. Part I: derivation of new constants. Canadian Mineralogist, 14, 498–502.

Mandarino, J.A. (1981) The Gladstone-Dale relationship. Part IV: the compatibility concept and its application. Canadian Mineralogist, 19, 441–450.

Mattson, S.M. and Rossman, G.R. (1984) Ferric iron in tourmaline. Physics and Chemistry of Minerals, 11, 225-234.

Novák, M., Povondra, P., and Selway, J.B. (2004) Schorl-oxy-schorl to dravite-oxy-dravite tourmaline from granitic pegmatites; examples from the Moldanubicum, Czech Republic. European Journal of Mineralogy, 16, 323-333.

Novák M., Škoda P., Filip J., Macek I., and Vaculovič T. (2011) Compositional trends in tourmaline from intragranitic NYF pegmatites of the Třebíč Pluton, Czech Republic; electron microprobe, Mössbauer and LA-ICP-MS study. Canadian Mineralogist, 49, 359-380.

Pouchou, J.L. and Pichoir, F. (1991) Quantitative analysis of homogeneous or stratified microvolumes applying the model "PAP." In K.F.J. Heinrich and D.E. Newbury, Eds., Electron probe quantitation, p. 31-75. Plenum, New York.

Razmanova, Z.P., Kornetova, V.A., Shipko, M.N., and Belov, N.B. (1983) Refinements in crystal structure and configuration of iron-bearing uvite. Trudy, Mineralogicheskiy Muzeya Akademiya Nauk SSSR, 31, 108-116 (in Russian)

Rozhdestvenskayaa, I.V., Setkovab, T.V., Vereshchagina, O.S., Shtukenberga, A.G., and Shapovalovb, Yu.B. (2012) Refinement of the Crystal Structures of Synthetic Nickel- and Cobalt-Bearing Tourmalines. Crystallography Reports, 57, 57-63.

Sheldrick, G.M. (2008) A short history of SHELX. Acta Crystallographica, A64, 112-122.

Skogby, H., Bosi, F., and Lazor, P. (2012) Short-range order in tourmaline: a vibrational spectroscopic approach to elbaite. Physics and Chemistry of Minerals, 39, 811-816.

Taran, M.N. and Rossman, G.R. (2002) High-temperature, high-pressure optical spectroscopic study of ferric iron-bearing tourmaline. American Mineralogist, 87, 1148-1153.

Taylor, M.C., Cooper, M.A., and Hawthorne, F.C. (1995) Local charge-compensation in hydroxyl-deficient uvite. Canadian Mineralogist, 33, 1215.1221.

van Hinsberg, V.J. and Schumacher, J.C. (2011) Tourmaline as a petrogenetic indicator mineral in the Haut-Allier metamorphic suite, Massif Central, France. Canadian Mineralogist, 49, 177-194.

van Hinsberg, V.J., Henry, D.J., and Marschall, H.R. (2011) Tourmaline: an ideal indicator of its host environment. Canadian Mineralogist, 49, 1-16.

Wright, S.E., Foley, J.A., and Hughes, J.M. (2000) Optimization of site occupancies in minerals using quadratic programming. American Mineralogist, 85, 524-531.

Žáček, V., Frýda, J., Petrov, A., and Hyršl, J. (2000) Tourmalines of the povondraite-(oxy)dravite series from the cap rock of meta-evaporite in Alto Chapare, Cochabamba, Bolivia. Journal of the Czech Geological Society, 45, 3-12.

459

460 **LIST OF TABLES**

472

473

474 **LIST OF FIGURES AND FIGURE CAPTIONS**

491 al. (2013), 2 oxy-schorl samples from Bačík et al. (2013). Black crosses represent
492 Co-rich and Ni-rich tourmalines from Rozhdestvenskayaa et al. (2012). Red
493 squares represent the ideal dravite, ideal oxy-dravite with ordered (O-) and
494 disordered (D-) formula (see text).

Table 1. Single-crystal X-ray diffraction data details for oxy-dravite

Crystal sizes (mm)	$0.20 \times 0.25 \times 0.30$
a (Å)	15.9273(2)
c (Å)	7.2001(1)
V (Å^3)	1581.81(4)
Range for data collection, 2θ (°)	5 - 69
Reciprocal space range *hkl*	$-22 \le h \le 25$
	$-25 \le k \le 25$
	$-11 \le l \le 11$
Total number of frames	3265
Set of measured reflections	7124
Unique reflections, R_{int} (%)	1586, 1.42
Completeness (%)	99.9
Redundancy	9
Absorption correction method	SADABS
Refinement method	Full-matrix last-squares on F^2
Structural refinement program	SHELXL-97
Extinction coefficient	0.0046(2)
Flack parameter	0.03(3)
*wR*2 (%)	3.33
*R*1 (%) all data	1.17
*R*1 (%) for $I > 2\sigma(I)$	1.16
GooF	1.140
Largest diff. peak and hole (±e$^-$/Å^3)	0.26 and –0.28

Notes: R_{int} = merging residual value; *R*1 = discrepancy index, calculated from *F*-data; *wR*2 = weighted discrepancy index, calculated from F^2-data; GooF = goodness of fit; Diff. Peaks = maximum and minimum residual electron density. Radiation, Mo*K*α = 0.71073 Å. Data collection temperature = 293 K. Space group *R*3*m*; *Z* = 3.

TABLE 2. Fractional atom coordinates and site occupancy for oxy-dravite (Å^2).

Site	*x*/*a*	*y*/*b*	*z*/*c*	Site occupancy
X	0	0	0.22939(18)	$Na_{0.914(5)}$
Y	0.12223(2)	0.061116(11)	0.63657(5)	$Al_{0.826(2)}Fe_{0.174(2)}$
Z	0.297683(16)	0.261493(17)	0.61014(4)	$Al_{1.00}$
B	0.10989(4)	0.21978(8)	0.45430(16)	$B_{1.00}$
T	0.191532(13)	0.189631(14)	0	$Si_{1.00}$
O1	0	0	0.7698(2)	$O_{1.00}$
O2	0.06076(3)	0.12151(6)	0.48724(12)	$O_{1.00}$
O3	0.26112(7)	0.13056(4)	0.50994(12)	$O_{1.00}$
O4	0.09356(3)	0.18712(6)	0.07152(12)	$O_{1.00}$
O5	0.18445(6)	0.09223(3)	0.09252(12)	$O_{1.00}$
O6	0.19447(4)	0.18433(4)	0.77729(9)	$O_{1.00}$
O7	0.28509(4)	0.28474(4)	0.07754(8)	$O_{1.00}$
O8	0.20920(4)	0.27005(4)	0.43936(9)	$O_{1.00}$
H3	0.2453(15)	0.1227(7)	0.396(3)	$H_{1.00}$

TABLE 3. Displacement parameters (Å^2) for oxy-dravite

Site	U^{11}	U^{22}	U^{33}	U^{23}	U^{13}	U^{12}	U_{eq}/U_{iso}*
X	0.0217(4)	0.0217(4)	0.0235(6)	0	0	0.0108(2)	0.0223(3)
Y	0.00895(14)	0.00675(11)	0.01145(14)	-0.00158(4)	-0.00316(8)	0.00448(7)	0.00881(9)
Z	0.00531(9)	0.00536(9)	0.00583(9)	0.00039(7)	-0.00008(7)	0.00262(7)	0.00552(5)
B	0.0054(3)	0.0060(4)	0.0076(4)	0.0005(3)	0.00027(16)	0.0030(2)	0.00626(17)
T	0.00458(8)	0.00429(8)	0.00590(8)	-0.00061(6)	-0.00054(6)	0.00226(6)	0.00490(5)
O1	0.0127(4)	0.0127(4)	0.0075(6)	0	0	0.00637(19)	0.0110(2)
O2	0.0112(3)	0.0042(3)	0.0098(4)	0.0009(2)	0.00044(12)	0.00210(15)	0.00918(15)
O3	0.0221(4)	0.0124(2)	0.0049(3)	0.00040(14)	0.0008(3)	0.0110(2)	0.01206(15)
O4	0.0070(2)	0.0140(4)	0.0094(3)	-0.0015(3)	-0.00075(13)	0.00699(18)	0.00936(14)
O5	0.0148(4)	0.0066(2)	0.0083(3)	0.00080(13)	0.0016(3)	0.00740(18)	0.00900(13)
O6	0.0090(2)	0.0089(2)	0.0054(2)	-0.00140(16)	-0.00081(16)	0.00505(18)	0.00751(10)
O7	0.0064(2)	0.0053(2)	0.0084(2)	-0.00106(17)	-0.00179(18)	0.00047(17)	0.00776(9)
O8	0.0039(2)	0.0088(2)	0.0140(2)	0.00227(18)	0.00051(18)	0.00275(19)	0.00909(10)
H3							0.018*

Notes: Equivalent (U_{eq}) and isotropic (U_{iso}) displacement parameters; H-atom was constrained to have a U_{iso} 1.5 times the U_{eq} value of the O3 oxygen.

TABLE 4. Selected bond distances (Å) for oxy-dravite.

B-O2	1.3760(14)	*Y*-O1	1.9397(8)
B-O8^{A} (× 2)	1.3740(8)	*Y*-O2^{B} (× 2)	1.9955(6)
<*B*-O>	1.375	*Y*-O3	2.1216(10)
		Y-O6^{C} (× 2)	1.9858(6)
T-O4	1.6246(3)	<*Y*-O>	2.004
T-O5	1.6396(4)		
T-O7	1.6030(6)	*Z*-O3	1.9985(5)
*T**-O6	1.6077(6)	*Z*-O6	1.9082(6)
<*T*-O>	1.619	*Z*-O8^{E}	1.8993(6)
		Z-O7^{E}	1.9073(6)
X-O2^{B,F} (× 3)	2.5012(12)	*Z*-O7^{D}	1.9572(6)
X-O4^{B,F} (× 3)	2.8201(10)	*Z*-O8	1.9258(6)
X-O5^{B,F} (× 3)	2.7284(10)	<*Z*-O>	1.933
<*X*-O>	2.683		
		O3-H	0.85(2)

Notes: Standard uncertainty in parentheses. Superscript letters: A = (*y* – *x*, *y*, *z*); B = (*y* – *x*, – *x*, *z*); C = (*x*, *x* – *y*, *z*); D = (*y* – *x* + 1/3, – *x* + 2/3, *z* + 2/3); E = (–*y* + 2/3, *x* – *y* + 1/3, *z* + 1/3); F = (–*y*, *x* – *y*, *z*). Transformations relate coordinates to those of Table 2.

* Positioned in adjacent unit cell.

TABLE 5. X-ray powder diffraction data for oxy-dravite

$I_{(meas)}$ (%)	$d_{(meas)}$ (Å)	$d_{(cal)}$ (Å)	h	k	l
44	6.377	6.383	1	0	1
25	4.978	4.979	0	2	1
14	4.598	4.595	3	0	0
67	4.222	4.221	2	1	1
64	3.983	3.980	2	2	0
84	3.483	3.484	0	1	2
10	3.379	3.377	1	3	1
9	3.011	3.008	4	1	0
100	2.963	2.962	1	2	2
7	2.898	2.896	3	2	1
7	2.622	2.621	3	1	2
68	2.576	2.575	0	5	1
19	2.400	2.400	0	0	3
14	2.377	2.376	2	3	2
14	2.343	2.342	5	1	1
8	2.190	2.189	5	0	2
9	2.163	2.162	4	3	1
13	2.128	2.128	0	3	3
15	2.056	2.055	2	2	3
35	2.041	2.040	1	5	2
6	2.019	2.018	1	6	1
52	1.915	1.918	3	4	2
7	1.876	1.876	1	4	3
6	1.849	1.848	6	2	1
5	1.785	1.785	1	0	4
18	1.660	1.660	0	6	3
25	1.633	1.640	2	7	1
11	1.593	1.592	5	5	0
2	1.528	1.532	9	0	0
14	1.507	1.507	0	5	4
8	1.504	1.504	8	2	0
4	1.481	1.481	2	4	4
14	1.456	1.456	5	1	4
6	1.432	1.430	7	4	0
6	1.418	1.417	6	5	1
11	1.410	1.410	4	3	4
6	1.329	1.329	3	5	4
5	1.310	1.309	10	1	0
9	1.276	1.277	5	0	5

Notes: $I_{(meas)}$ = measured intensity, $d_{(meas)}$ = measured interplanar spacing; $d_{(calc)}$ = calculated interplanar spacing; *hkl* = reflection indices. Estimated errors in $d_{(meas)}$-spacing range from 0.01 Å for large *d*-values to 0.001 Å for small *d*-values.

TABLE 6. Chemical composition of oxy-dravite

	Weight %		Apfu
SiO_2	37.01(10)	Si	5.98(5)
TiO_2	0.14(3)	Ti^{4+}	0.017(4)
B_2O_3*	10.76	B	3.00
Al_2O_3	33.11(20)	Al	6.31(5)
Fe_2O_3†	5.00	Fe^{3+}	0.61(1)
FeO†	0.19	Fe^{2+}	0.025(3)
MgO	8.56(8)	Mg	2.06(2)
Na_2O	2.65(3)	Na	0.83(1)
K_2O	0.10(1)	K	0.021(1)
H_2O*	2.65	OH	3.24
Total	100.58		

Notes: number of ions calculated on basis of 31 (O, OH, F). Uncertainties for oxides (in brackets) are standard deviation of 10 spots. B_2O_3 and H_2O uncertainty assumed at 5%. Standard uncertainty for ions was calculated by error-propagation theory.

* Calculated by stoichiometry.

† Determined by Mössbauer spectroscopy, $(FeO)_{EMPA}$ = 4.69(9).

TABLE 7. Site populations (*apfu*), site scattering factors (*epfu*) and mean bond lengths (Å) for oxy-dravite

Site	Site population	Site scattering		Mean bond length	
		refined	calculated	refined	calculated*
X	0.83 Na + 0.02 K + 0.15 □	10.05(5)	9.53		
Y	1.34 Al + 1.03 Mg + 0.58 Fe^{3+} + 0.03 Fe^{2+} + 0.02 Ti *(1.20 Al + 1.16 Mg + 0.60 Fe^{3+} + 0.03 Fe^{2+} + 0.02 Ti)***	45.8(1)	46.0	2.004	2.002
Z	4.94 Al + 1.03 Mg + 0.02 Fe^{3+} *(5.11 Al + 0.90 Mg)***	78†	77.3	1.933	1.931
T	5.98 Si + 0.02 Al *(6.00 Si)***	84†	84	1.619	1.619
B	3.00 B	15†	15	1.375	1.374
O3	3.00 (OH)	24†	24		
O1	0.76 O + 0.24 (OH)	9†	9		

Notes: O2, O4…O8 sites are fully populated by O^{2-}; apfu = atoms per formula unit; epfu = electrons per formula unit.

* Calculated from the ionic radii (Bosi and Lucchesi 2007).

** Site populations optimized by the procedure of Wright et al. (2000).

†Fixed in the final stages of refinement.

TABLE 8. Bond valence calculations (valence unit) for oxy-dravite

Site	*X*	*Y*	*Z*	*T*	*B*	BVS
O1		$0.51^{\times 3}\rightarrow$				1.53
O2	$0.15^{\times 3}\downarrow$	$0.44^{\times 2}\downarrow\rightarrow$			0.99	2.01
O3		0.31	$0.40^{\times 2}\rightarrow$			1.11
O4	$0.07^{\times 3}\downarrow$			$1.00^{\times 2}\rightarrow$		2.06
O5	$0.08^{\times 3}\downarrow$			$0.96^{\times 2}\rightarrow$		2.00
O6		$0.45^{\times 2}\downarrow$	0.51	1.04		2.00
O7			0.51	1.06		2.02
O8			0.45 0.49 0.52		$0.99^{\times 2}\downarrow$	2.00
BVS	0.91	2.59	2.87	4.06	2.97	
MFV*	0.85	2.65	2.83	4.00	3.00	

* MFV = mean formal valence from site populations

TABLE 9. Comparative data for oxy-dravite, fluor-dravite and dravite.

	Oxy-dravite	Fluor-dravite	Dravite
	$Na(Al_2Mg)(Al_5Mg)Si_6O_{18}(BO_3)_3(OH)_3O$	$NaMg_3Al_6Si_6O_{18}(BO_3)_3(OH)_3F$	$NaMg_3Al_6Si_6O_{18}(BO_3)_3(OH)_3(OH)$
a (Å)	15.9273(2)	15.955(3)	15.96(2)
c (Å)	7.2001(1)	7.153(2)	7.21(2)
V (Å^3)	1581.81(4)	1576.9(6)	1590.5
Space group	*R*3*m*	*R*3*m*	*R*3*m*
Optic sign	Uniaxial (–)	Uniaxial (–)	Uniaxial (–)
ω	1.650(5)	1.645(2)	1.634 - 1.661
ε	1.620(5)	1.621(2)	1.612 - 1.632
Colour	Dark red	Blackish brown	Pale brown to dark-brown to brownish-black, dark-yellow, blue
Pleochroism	O = orange E = pink	O = pale yellow-brown E = colorless	O = pale yellow E = colorless, yellowish, greenish, brownish
Reference	This work	Clark et al. (2011)	www.mindat.org

TABLE 10. Selected tourmaline formulae.

Name	Representative formula	Substitution related to oxy-dravite
Oxy-dravite	$Na^{Y}(Al_2Mg)^{Z}(Al_5Mg)Si_6O_{18}(BO_3)_3(OH)_3O$	
Oxy-schorl	$Na^{Y}(AlFe^{2+}{}_2)^{Z}(Al_6)Si_6O_{18}(BO_3)_3(OH)_3O$	$Fe^{2+} \rightarrow Mg^{2+}$
Oxy-chromium-dravite	$Na^{Y}(Cr_3)^{Z}(Cr_4Mg_2)Si_6O_{18}(BO_3)_3(OH)_3O$	$Cr^{3+} \rightarrow Al^{3+}$
Oxy-vanadium-dravite	$Na^{Y}(V_3)^{Z}(V_4Mg_2)Si_6O_{18}(BO_3)_3(OH)_3O$	$V^{3+} \rightarrow Al^{3+}$
Povondravite	$Na^{Y}(Fe^{3+}{}_3)^{Z}(Fe^{3+}{}_4Mg_2)Si_6O_{18}(BO_3)_3(OH)_3O$	$Fe^{3+} \rightarrow Al^{3+}$

This is a preprint, the final version is subject to change, of the American Mineralogist (MSA)
Cite as Authors (Year) Title. American Mineralogist, in press.
(DOI will not work until issue is live.) DOI: http://dx.doi.org/10.2138/am.2014.4441

Figure 1a

This is a preprint, the final version is subject to change, of the American Mineralogist (MSA)
Cite as Authors (Year) Title. American Mineralogist, in press.
(DOI will not work until issue is live.) DOI: http://dx.doi.org/10.2138/am.2014.4441

Figure 1b

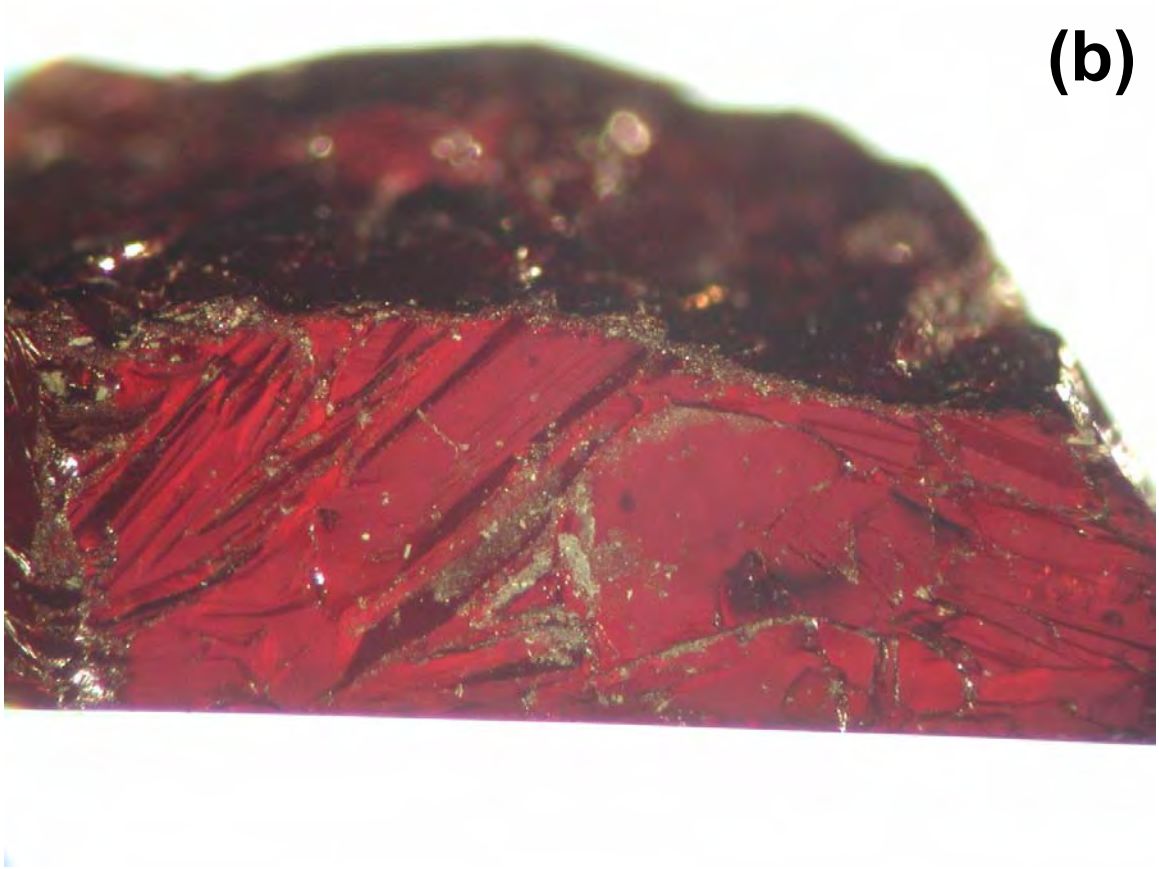

Figure 2

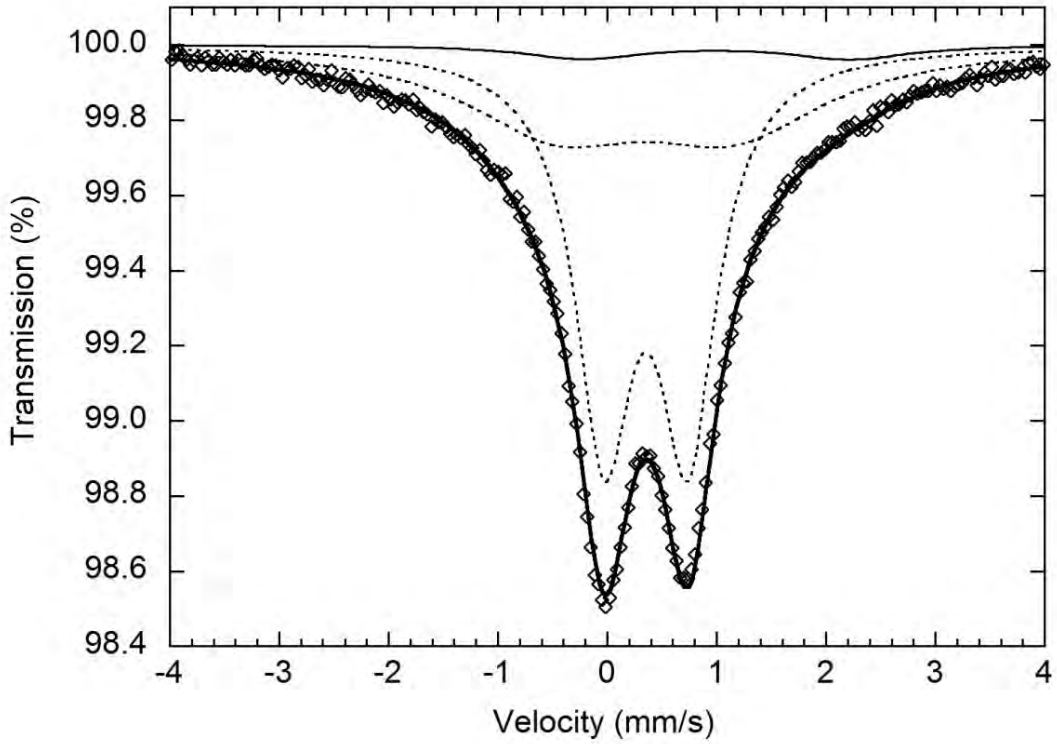
100.0
99.8
99.6
99.4
99.2
99.0
98.8
98.6
98.4
Transmission (%)
-4
-3
-2
-1
0
1
2
3
4
Velocity (mm/s)

This is a preprint, the final version is subject to change, of the American Mineralogist (MSA)
Cite as Authors (Year) Title. American Mineralogist, in press.
(DOI will not work until issue is live.) DOI: http://dx.doi.org/10.2138/am.2014.4441